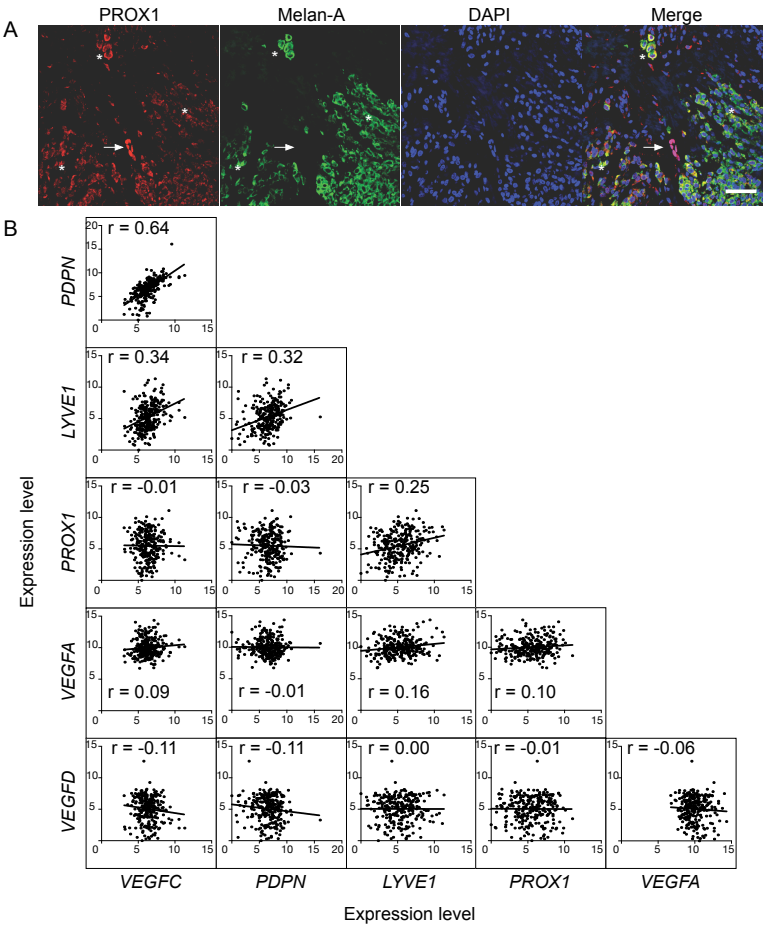

Supplemental Figure 1. Correlation of lymphatic markers from human metastatic melanoma samples. **A.** Immunofluorescence detection of PROX1^{+}Melan-A^{+} cells in primary human cutaneous melanoma. Nuclear PROX-1 staining consistent with lymphatic vessel staining (Melan-A^{-}, arrow) and cytoplasmic staining in Melan-A^{+} cells (*). PROX1, red; Melan-A, green; DAPI, blue. Scale bar = 50μm. **B.** Correlation of lymphatic markers (*LYVE1, PDPN, PROX1*) with eachother and with vascular endothelial growth factor genes (*VEGFA*, *VEGFB*, *VEGFC*, *VEGFD*). 266 metastatic cutaneous melanoma samples from the Broad Institute's TCGA database. Pearsons correlation coefficient (r).

Supplemental Figure 2

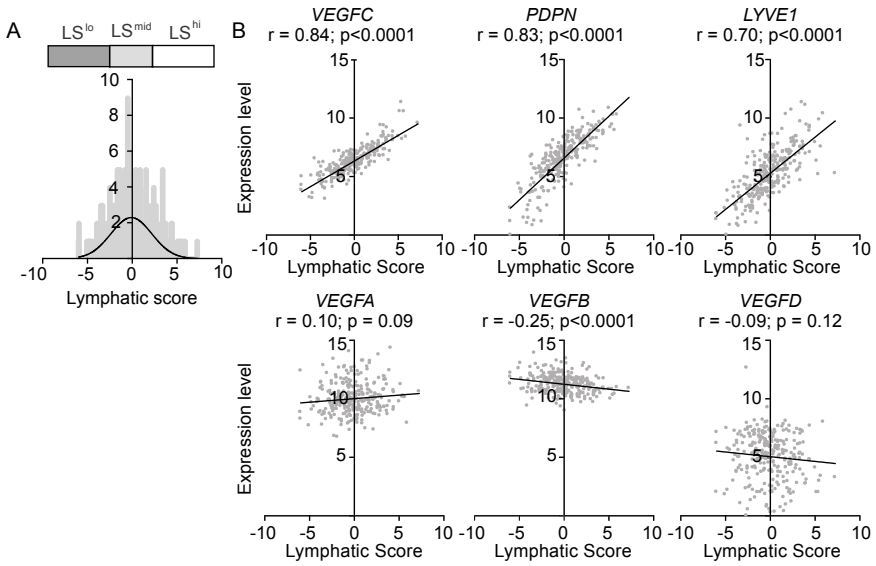

Supplemental Figure 2. The lymphatic score correlates with the lymphangiogenic growth factor *VEGFC* and not *VEGF A,B* or *D*. **A**. Distribution of lymphatic scores. **B**. Correlation of lymphatic score (LS) with *VEGFC*, *PDPN*, *LYVE1*, *VEGFA*, *VEGFB*, and *VEGFD* expression in 266 metastatic cutaneous melanoma samples. Pearsons correlation coefficient (r).

Supplemental Figure 3

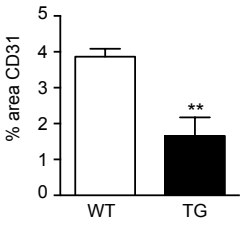

Supplemental Figure 3. Quantification of percent area of CD31 staining. **A**. Quantification of percent area of $CD31^+$ pixels quantified over total image area from immunohistochemical staining in paraffin sections. Data represented as mean ± SEM, n=3, **p<0.05.

Supplemental Figure 4

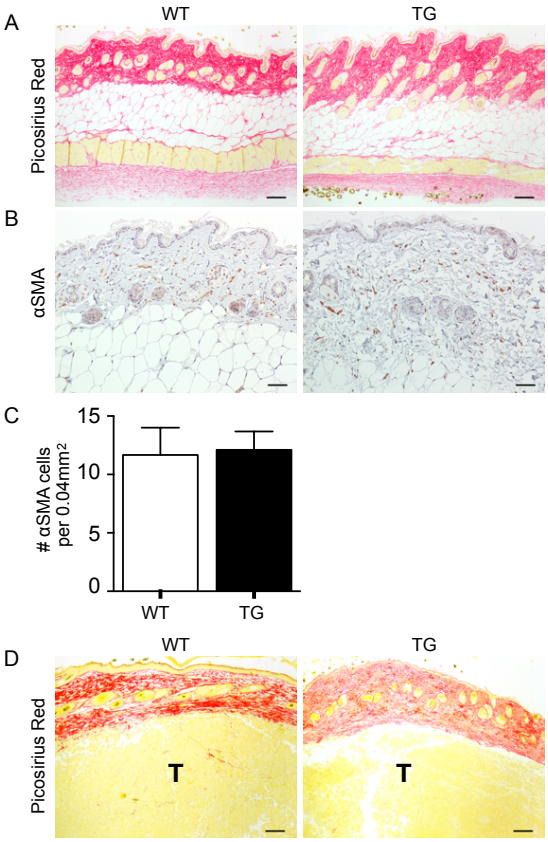

Supplemental Figure 4. K14-VEGFR3-Ig mice do not exhibit enhanced cutaneous fibrosis as compared to wildtype littermates. **A**. Picosirius Red staining was performed on skin taken from naive wildtype (WT) and K14-VEGFR3-Ig (TG) mice. Collagen fibers are stained red; scale bar = 100μm. **B**. Immunohistochemistry for α-SMA in naïve skin from WT and TG mice (scale bar = 50μm) and **C**. quantification of number of α-SMA^{+} cells per 0.04mm^{2}; n=3. Data represented as mean ± SEM, n=3. **D**. Picosirius Red staining in B16F10 tumor implanted intradermal in WT and TG mice. Scale bar = 100μm; "T" marks tumor.

Supplemental Figure 5

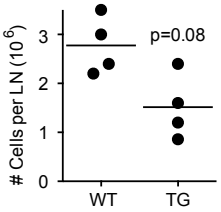

Supplemental Figure 5. Lymph node cellularity in wildtype and K14-VEGFR3-Ig mice. Brachial lymph node cellularity (naïve) in WT and TG mice, n=4. P-values were obtained with Student's unpaired t test.

Supplemental Figure 6

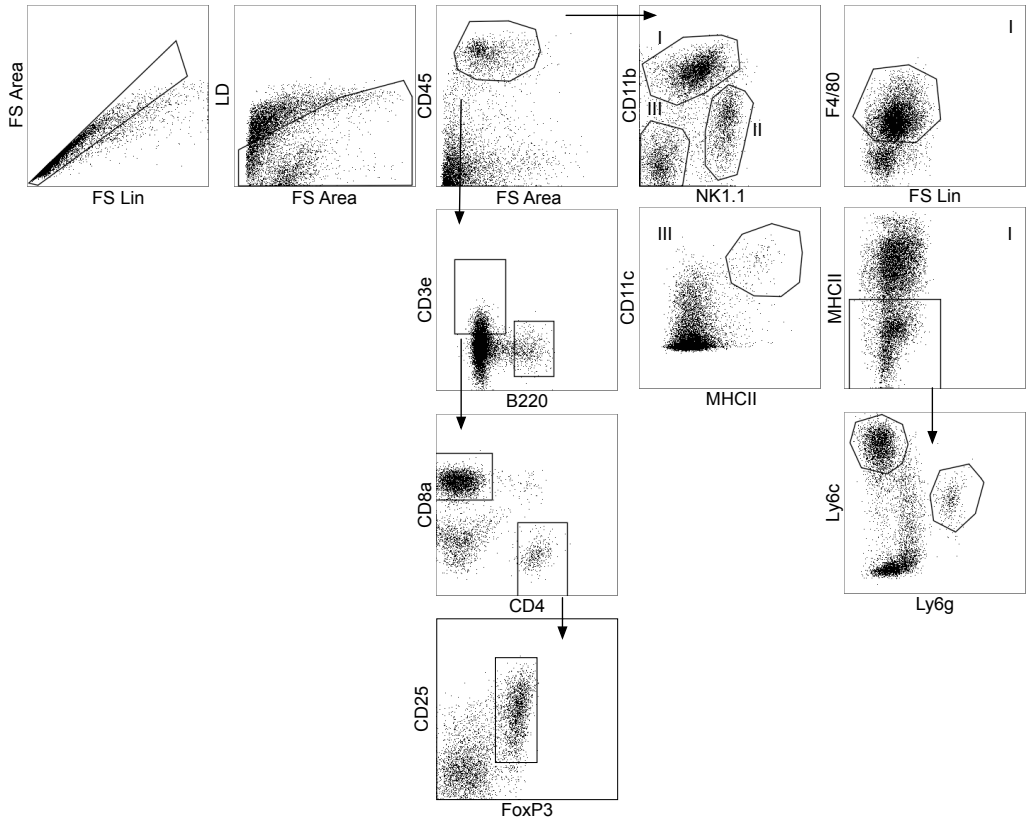

Supplemental Figure 6. Gating scheme for analysis of infiltrating immune populations by flow cytometry. Multi-color flow cytometry gating scheme to quantify immune populations in tumor, spleen and draining lymph node. Representative plots from the tumor of wildtype mouse.

Supplemental Figure 7

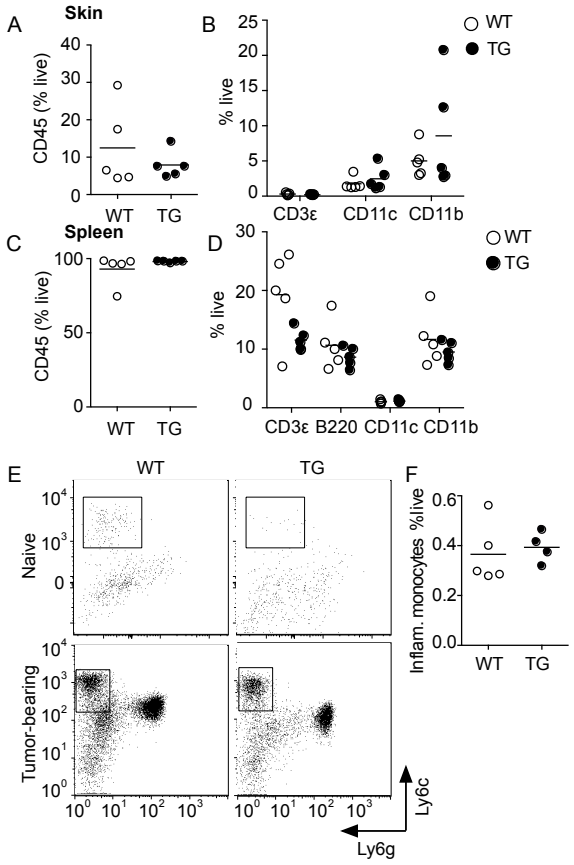

Supplemental Figure 7. Homeostatic cutaneous immune populations in wildtype and K14-VEGF3-Ig mice. Naïve skin and spleens were digested and analyzed by flow cytometry for immune populations from wildtype (WT) and K14-VEGFR3-Ig (TG) mice. **A**. Total $CD45^+$ cells as a percent of live cells and **B**. CD3ε, CD11c and CD11b cells as a percent of $CD45^+$ cells are quantified from the skin and **C** and **D**. spleens of mice. **E**. Representative plots of $Ly6c^+$ and $Ly6g^+$ populations in spleens of naïve and tumor-bearing mice and **F**. quantification of % $Ly6c^+Ly6g^-$ inflammatory monocytes in naïve spleens, n≥4. Quantification of tumor-bearing mice in Figure 3. Gated on $CD45^+CD11c^-CD11b^+F4/80^-$ inflammatory monocytes.

Supplemental Figure 8

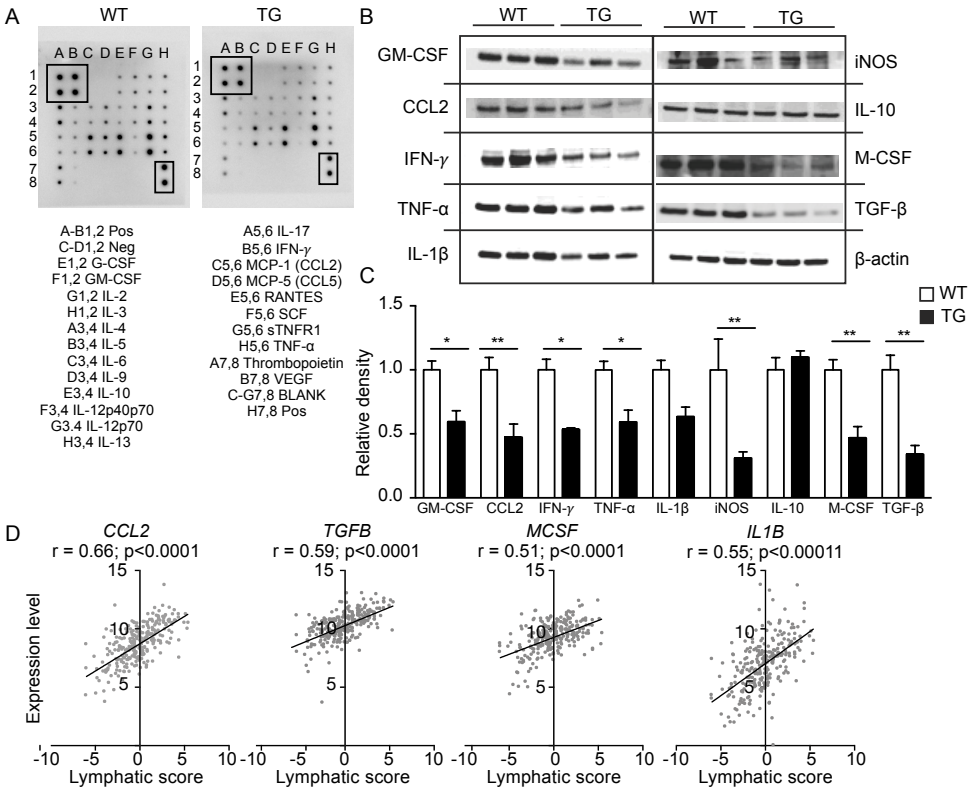

Supplemental Figure 8. Correlation between lymphatic involvement and intratumoral cytokine expression. **A.** Representative blot (above) and key (below) from cytokine array, n=7. Black squares indicate control IgG spots used for relative intensity calculations. Quantification presented in Figure 3. **B**. Representative western blots on tumor lysate and **C**. quantification of optical density normalized to WT (n=3); data are represented as mean ± SEM. P-values were obtained with Student's unpaired t tests of values. *p<0.05, **p<0.01. **D**. Representative plots correlate expression of key cytokines (*CCL2*, *TGFB*, *MCSF*, *IL1B*) with lymphatic score in 266 cutaneous metastatic melanoma samples from the Broad Institute TCGA database. Pearsons correlation coefficient (r).

Supplemental Figure 9

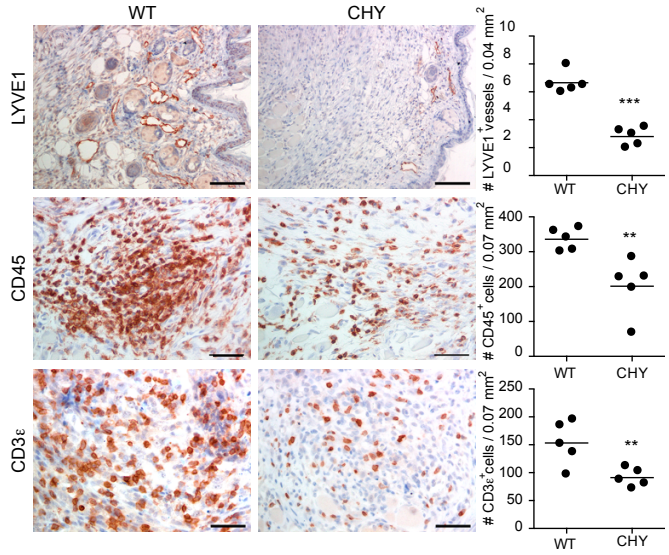

Supplemental Figure 9. *Chy* mice demonstrate decreased dermal lymphatic vessel density and leukocytic infiltrate. C3BHA syngeneic breast carcinoma cells were injected intradermal (n=5) into ears of *Chy* mice harboring an inactivating mutation in the tyrosine kinase domain of VEGFR3. Lymphatic vessel density (LYVE1; 20x scale bar=100μm) and leukocytic infiltrate (CD45 and CD3ε; 40x scale bar=50μm) were evaluated by immunohistochemistry (left) and quantified as number per area (right). P-values were obtained with Student's unpaired t tests of values. **p≤0.01 ***p<0.001.

Supplemental Figure 10

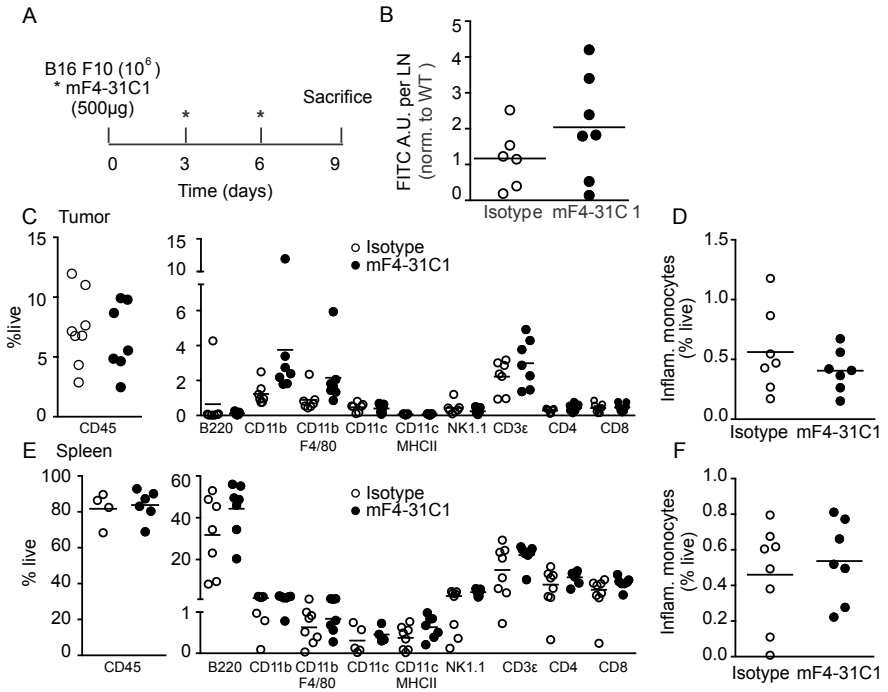

Supplemental Figure 10. Inhibition of VEGFR3 signaling during tumor progression is insufficient to suppress local inflammation in wildtype mice. **A**. B16F10 tumors were implanted into wildtype mice and treated with either VEGFR3 neutralizing antibody (mF4-31C1, Eli Lilly and Company, 500µg) or rat IgG isotype control on day 0, 3 and 6 to inhibit active VEGF-C signaling during tumor development. **B.** Fluid drainage was assessed by intratumoral injection of 70kDa FITC dextran and analysis of tumor draining lymph node 30 min later. (n=5) Relative numbers of tumor-associated **C**. $CD45^+$ cell populations and **D**. inflammatory monocytes ($CD11c^-CD11b^+F4/80^-Ly6c^{hi}Ly6g^-$), quantified as a percent of live cells in the tumor. Relative numbers of splenic (**E**) $CD45^+$ cell populations and **F**. inflammatory monocytes ($CD11c^-CD11b^+F4/80^-Ly6c^{hi}Ly6g^-$) (n=5). Data represented as mean ± SEM.